

Ultra compact optics for optical wireless communications

Juan C. Miñano, Pablo Benítez, Rubén Mohedano, José L. Alvarez, Maikel Hernández, Juan C. González*, Kazutoshi Hirohashi**, Satoru Toguchi**

IES, E.T.S.I. Telecomunicación, Universidad Politécnica de Madrid, 28040 Madrid, Spain

*Universidad Europea de Madrid, Villaviciosa de Odón, Madrid, Spain

**HITS (High Speed Infrared Transmission Systems) Laboratories, Inc., 2-16-16 Chuourinkan, Yamato, 242-0007 Japan

ABSTRACT

Advanced optical design methods [J.C. Miñano, J.C. González, “New method of design of nonimaging concentrators”, Appl. Opt. 31, 1992, pp.3051-3060] using the keys of nonimaging optics lead to some ultra compact designs which combine the concentrating (or collimating) capabilities of conventional long focal length systems with a high collection efficiency [J.C. Miñano, J.C. González, P. Benítez, “A high gain, compact, nonimaging concentrator: the RXI”, Appl. Opt. 34, 1995, pp. 7850-7856] [J.C. Miñano, P. Benítez, J.C. González, “RX: a nonimaging concentrator”, Appl. Opt. 34, 1995, pp. 2226-2235]. One of those designs is the so-called RXI. Its aspect ratio (thickness/aperture diameter) is less than 1/3. Used as a receiver, i.e. placing a photodiode at the proper position, it gets an irradiance concentration of the 95% of the theoretical thermodynamic limit (this means for example, a concentration of 1600 times with an acceptance angle of ± 2.14 degrees). When used as an emitter (replacing the aforementioned photodiode by an LED, for instance), similar intensity gains may be obtained within an angle cone almost as wide as the 95% of the thermodynamic limit. In a real device these irradiance (and intensity) gains are reduced by the optical efficiency. This combination of high concentration factors, relatively wide angles, simplicity and compactness make the optical device almost unique. This work will show the results of the measurements done with several RXI prototypes of 40-mm aperture diameter, all of them made of PMMA (by injection process).

Keywords: Nonimaging optics, compact optics, optical wireless link.

1. INTRODUCTION

Geometrical Optics development has been intimately linked to Imaging Optics since its very beginning. The reasons for this are obvious: the imaging problem involves a great variety of applications in many industrial and commercial activities. It was not until the 60's when it was recognized that the image formation constrain is not needed to solve some optical design problems, and in particular the problem of maximum radiation transfer between a source and a target. The elimination of this constrain led to an additional degree of freedom which was cleverly used to get more effective designs, i.e., to get more efficient and much simpler designs. This new branch of Optics was called Nonimaging Optics. The beginning of this activity can be located with the invention of the Compound Parabolic Concentrator (CPC). Three independent teams invented the CPC, one in the University of Chicago, one in the former USSR, and other one in Germany. The contributions to the field done by US team, leaded by Prof. Winston, make it to stand out immediately. One of these contributions (a milestone in the theoretical formulation of Nonimaging Optics) was the so-called Edge Ray Principle, which is the basis of any existing method of design of Nonimaging devices. A classical book in this field is given in reference ¹ and its current status can be viewed in the Proceedings of “Nonimaging Optics: Maximum-Efficiency Light Transfer” SPIE conferences whose fifth edition has been held last July in Denver.

Because image formation is of no interest in the design of nonimaging devices, the mathematical tools of nonimaging optics look a bit odd from the imaging optics point of view: aberrations have no interest, paraxial approximations are useless, concepts like focal length, numerical aperture, principal planes loose their significance for a nonimaging device. By other side optical invariants (and in particular the etendue conservation) are extensively used in nonimaging optics (without paraxial approximation), other concepts like the Poisson brackets which seems to belong exclusively to Mechanics play its role in nonimaging optics and new definitions appear: geometrical vector flux, flow lines, density of etendue per unit of skewness, etc. Consequently, the methods of design differ strongly from the imaging ones.

The main applications of Nonimaging Optics are in light (radiation) transfer: Illumination, Solar Energy, Light Pumping, etc. In all these cases, the radiation of a source has to be transferred with maximum efficiency to a given target. This is also the case in Wireless Optical Links, both for emission and for reception of signals. Let us consider an example: an optical device has to be designed to concentrate on a photodiode the radiation coming from a distant source while making allowance for an angular aiming error of $\pm\theta_s$. We call the device a concentrator. The photodiode surface has to be as small as possible in order to reduce internal noise and to minimize switching time, both of which depend on the photodiode area. Assume that the concentrator is illuminated by the source with intensity I_s (in mW/mm^2 , for instance) and that its entry aperture area is A_e . For simplicity we are also going to assume that the problem has rotational symmetry and that there are no reflection, absorption or dispersion losses. In order to get the less expensive concentrator it is desirable that all the radiation impinging the entry aperture within an angle θ such that $\theta \leq \theta_s$ is directed to the photodiode. If we define $T(\theta)$ as the ratio of power reaching the photodiode surface to the power impinging the aperture at a given angle θ , the preceding condition can be written as $T(\theta)=1$ when $\theta \leq \theta_s$. Owing to the energy conservation principle, $T(\theta) \leq 1$. There is not a direct relationship between the cost of the optical component and the value of $T(\theta)$ when $\theta \leq \theta_s$, but the trend towards cheapest concentrators is to design them as small as possible, and their size is intimately linked with the entry aperture area. From the conservation of etendue¹ (also known as the brightness conservation) it can be concluded that the photodiode area fulfils the following inequality:

$$A_p \geq A_e \frac{\sin^2(\theta_s)}{n^2} \quad (1)$$

where n is the refractive index of the medium surrounding the photodiode surface. The equality in (1), i.e., the smallest photodiode area, can only be achieved if $T(\theta)=1$ when $\theta \leq \theta_s$ and $T(\theta)=0$ when $\theta > \theta_s$. This means that the angular transmission $T(\theta)$ must have a sharp cut-off when $\theta = \theta_s$.

This is not a problem for an imaging design. Assume that θ_s is small. If the photodiode is placed at the focal plane of a thin lens (see Figure 1), a sharp cut-off is obtained when $\theta = \theta_s$ if the photodiode diameter is the $2 f \tan(\theta_s)$ (f is the lens focal length). Let D_e be the entry aperture diameter, then

$$A_p = 4 A_e \left(\frac{f}{D_e} \right)^2 \tan^2(\theta_s) \quad (2)$$

High-aperture camera lenses, much more complex than a simple thin lens, have f/D_e ratios of about 1. Considering a refractive index material $n=1.5$ (this is a value achieved and surpassed by most of the practical encapsulation materials), the photodiode area in (2) is still 9 times greater than the lower bound (1). Smaller photodiode areas can be achieved with imaging systems containing reflectors. Nevertheless, simple (and inexpensive) imaging designs fall a long way short of the lower bound in (1). A more extensive discussion about the feasibility of imaging devices as concentrators can be found in reference¹.

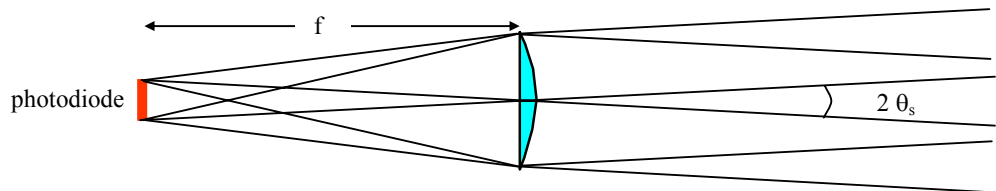


Figure 1. Thin lens concentrating the beam $\pm\theta_s$ on the photodiode surface

The equality in (1) can only be achieved if any point of the receiver is illuminated isotropically when the concentrator's entry aperture is illuminated homogeneously in the angular cone $\theta \leq \theta_s$. This is the reason why, generally speaking, imaging devices does not perform well as concentrators. By other side, the photodiode is almost insensitive to the light distribution and so image formation is useless. We are interested in collecting the beam coming from directions contained in $\pm\theta_s$, but the distribution of the rays on the photodiode surface is worthless. This difference between the objectives of image formation and nonimaging devices is shown in Figure 2

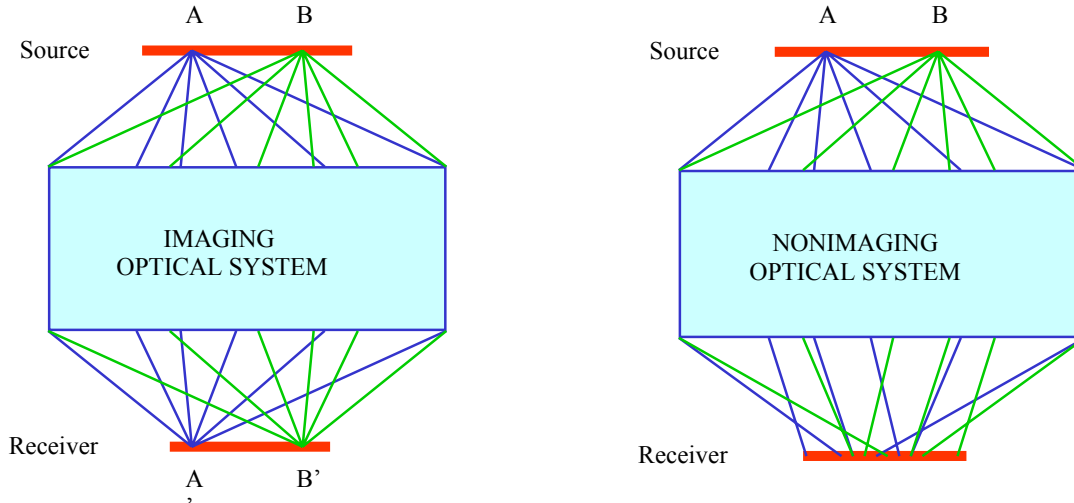


Figure 2. Rays emerging from A (B) are focused on A' (B') in an imaging system. Imaging formation is worthless in a nonimaging optical system whose goal is the maximum efficiency of light transfer.

2. NONIMAGING DESIGN METHODS

There are basically three design methods for nonimaging devices. All of them are based on the edge ray principle and are within the framework of Geometrical Optics. From one of them (the Poisson bracket method^{2,3,4}) only devices with continuously variable refractive index have been designed. For this reason, the concentrators are costly and we are not going to consider them here.

2.1. The Winston-Welford method

The first method, that we call the Winston-Welford method, was developed in the 60's and 70's. Full explanation of it is given in reference¹. The most characteristic device derived from this method is the CPC (Compound Parabolic Concentrator) whose cross-section is shown in Figure 3. This cross-section consist of two parabolic reflectors such that the axis of one of the parabolas is tilted $\theta_s' = \sin^{-1}(\sin \theta_s/n)$ (the other one is tilted $-\theta_s'$) with respect the axis of symmetry (z axis) and its focus is at one of the receivers edge. In this way, the rays impinging the entry aperture with incidence angles $\pm\theta_s$ and contained on the paper plane are focused on both edges of the receiver, as it is shown in Figure 3 for some of them. The set of rays impinging the entry aperture with an incidence angle equal to θ_s (with respect to the z axis) is called the edge ray set.

The CPC filled with any dielectric material ($n>1$) and with rotational symmetry almost gets the lower bound of equation (1). The ratio A_e/A_p is closer than 95% to the limit for small values of θ_s (<1 degree) and increases to 100% when θ_s goes to 90 degrees. Additionally, the CPC is a simple device. For small enough values of θ_s or high enough values of the refractive index n , the reflection on the lateral parabolas can be achieved by total internal reflection and thus no metallic reflector is needed.

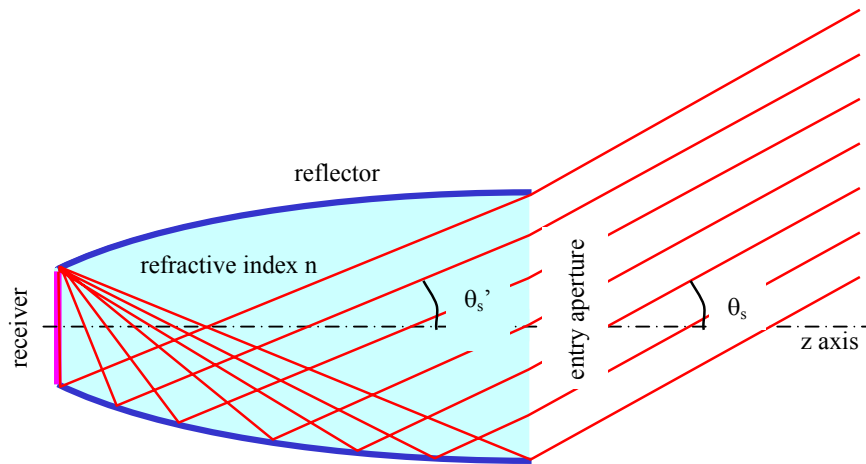


Figure 3. The Compound Parabolic Concentrator is designed to collect all the radiation impinging its entry aperture within the angle $\pm\theta_s$, and to concentrate it on the receiver.

The same design procedure can be used for other receiver shapes, or different input bundles. For instance, if the input bundle is formed by the rays impinging the entry aperture and coming from a certain flat source placed at a finite distance from the concentrator, the device obtained is called CEC (Compound Elliptic Concentrator). If the input bundle is a generalized 2D bundle of rays, the method can also be applied with success (in this case the method is sometimes called Tailored Edge Rays). This method of design is 2D, i.e., the design is done just considering the rays contained in the meridian plane. For these rays, the concentrator is ideal. The 3D concentrator is obtained by rotational symmetry around the z-axis. A ray-tracing analysis of the 3D design is needed to identify the bundle of rays reaching the receiver (bundle of collected rays). Linear (cylindrical) concentrators are designed in a similar way, i.e., they are designed with linear symmetry from the 2D design.

The concentrators obtained by this method use to be very deep (z dimension) when θ_s is small, or, in general, when the angular span on the input bundle is small. For such applications, combinations of imaging and nonimaging concentrators are very convenient. The imaging component is used as a first stage of concentration taken advantage of the ability of such devices to obtain a sharp cut-off angular response with a moderate size. The real or virtual receiver of this first stage of concentration is the source for the second one. The second stage of concentration is done with a nonimaging concentrator, which achieves (or almost achieves) the lower bound of concentration of equation (1) with a reasonable size. Thus, the goal of the imaging part is to get the sharp cut-off angular response and that of the nonimaging part is to get the lower bound of the receiver size.

Figure 4 shows one of these imaging and nonimaging combinations. The first stage is a parabolic mirror that focuses the incoming bundle in the virtual receiver located at the parabola focal plane. This virtual receiver is the source for the second stage of concentration, which in this case is a Flow Line Concentrator (FLC). The FLC concentrates further the beam on the actual receiver, which is located in the same plane as the virtual one but is smaller in size. The FLC, unlike the rotational CPC, has the property of achieving the theoretical limit of concentration in 3D geometry (reference ¹). Similar imaging and nonimaging combinations have been used, for instance, for concentrating sun radiation to levels higher than the ones at the sun's surface⁵ (and, of course, still fulfilling the 2nd Principle of Thermodynamics).

These combinations have an additional property, which is interesting for wireless optical communications: With some minor exceptions, nonimaging concentrators are based on non-conventional aspheric surfaces. The technologies available for the replication of such surfaces give less accuracy, for the same cost, than the ones obtained in the spherical case or, more generally, than the ones needed in the manufacture of imaging devices. This is because, the technology for manufacturing imaging devices, based on spherical or aspheric surfaces, is highly developed. Broadly speaking, the performance of a concentrator depends on the ratio of the optical surface slope error and the angular span of the collected beam at any point of the concentrator⁶. In applications such the ones found in long distance wireless optical communication, the bundle span is very small at the concentrator's entrance and must be very wide (isotropic illumination of the receiver) if minimum receiver area is required. In this case, the imaging and nonimaging combination offers a way of minimizing the ratio of optical

surface slope error to angular span. The bundle should intercept the imaging part when the angular span is small and the nonimaging part when the angular span is wide, as in the case shown in Figure 4. This fits well with the functional sharing between imaging and nonimaging part described before.

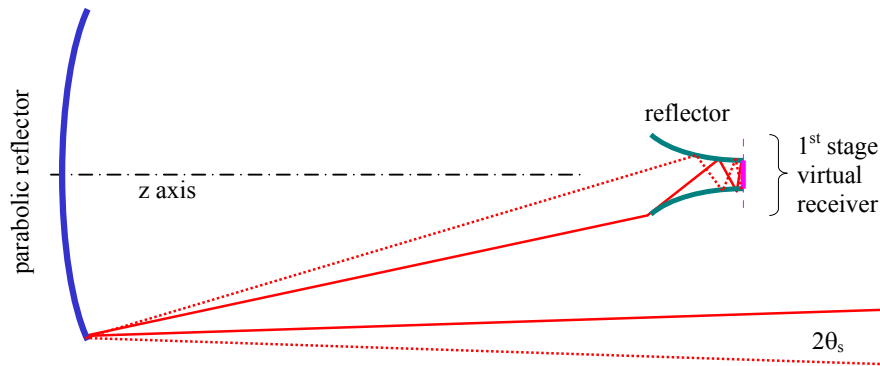


Figure 4. Combination of a parabolic mirror and a FLC (Flow Line Concentrator) showing also the trajectories of two edge rays (not to scale).

2.2. The SMS method

During the 90's a new method of design of nonimaging concentrators was developed^{7, 8, 9, 10}. The devices generated with this method (called Simultaneous Multiple Surface method, SMS) show four important characteristics:

1. High efficiency: For small values of the input bundle angular span θ_s (<10 degrees) the concentrators are closer than 96% to the lower bound of equation (1).
2. Compactness: The aspect ratio (device thickness/aperture diameter) is as small as 0.27, even for small values of θ_s .
3. No parts close to the receiver (emitter): Unlike the CPC, or any other concentrator designed with the previously described method, whose reflectors end at the receiver (emitter) edges, there is no optical surface in contact with the receiver (emitter).
4. Simplicity: The devices are very simple, and in most of the cases, can be manufactured in a single solid piece.

The interest of point 3 should be clarified a bit more. As seen in Figures 3 and 4 the reflectors end at the receiver's edges. This is sometimes a problem for several reasons: if the receiver is an optoelectronic component some electrical contacts have to be extracted through this part of the reflectors. If the concentrator uses dielectric material to get a higher concentration, this has to be glued to the receiver and the spare glue will flow to the reflectors, canceling total internal reflection if it is used. If what we have is a thermal receiver (solar energy applications) the reflectors add a way for heat losses. Reference¹¹ gives a solution for this problem based on the SMS method (for cylindrical receivers).

The different optical surfaces of a device derived from the SMS method are designed altogether. The method can be combined with the previous one to obtain mixed devices^{12,13}.

The first SMS device was a lens^{7,8}, which proved that optical devices sharply focusing 2 bundles can be designed provided that the degrees of freedom for the design are at least the ones given by two surfaces. Devices with a single surface and focusing a single beam were already known since the time of Descartes¹⁴. This result has been recently proved to be also valid for 3D geometry¹⁵.

Next section is devoted to introduce two devices designed with the SMS method, the RX and the RXI. They are not the only ones but their properties can summarize the aspects more interesting for wireless optical communications.

3. TWO SMS DEVICES: RX AND RXI

The RX is a simple device with two optical surfaces: a dioptric (a refractive surface) and a reflector (see Figure 5). Thus it can be manufactured in a single dielectric piece. The theoretical profiles of both curves, which are calculated numerically, have not an analytical expression. As a concentrator of radiation, the rays coming from the source are refracted in the dioptric and then reflected in the mirror to be finally sent to the receiver. This is a flat circle whose active side is facing the reflector. Its aspect ratio (concentrator thickness to aperture diameter ratio) is smaller than 0.5 for designs like the one shown in Figure 5.

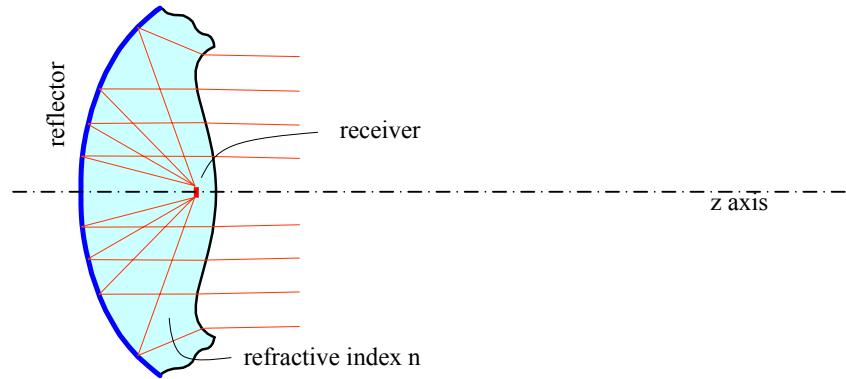


Figure 5. RX concentrator is just a single dielectric piece with a mirrored surface. It achieves up to a 98% of the maximum theoretical concentration with a thickness to diameter ratio < 0.5 . Refractive index 1.5

Although the RX has been designed with the SMS method, which is a nonimaging method, the RX shows some impressive imaging characteristics¹⁶. This is not contradictory since nonimaging designs don't impose the imaging formation condition but neither impose a no imaging formation condition. Thus the RX is a good imaging and nonimaging device at the same time (this is not new, the graded index lens called Luneburg lens¹⁷ is a perfect imaging and nonimaging device), i.e., it forms image with surprisingly high concentration (98% of the theoretical maximum). Figure 6 shows a comparative example. The RX of this figure forms image with the same quality as a conventional plano-convex lens $f/4.5$. The same quality here meaning that the Modulation Transfer Function (MTF) of both devices is approximately equal. Nevertheless,

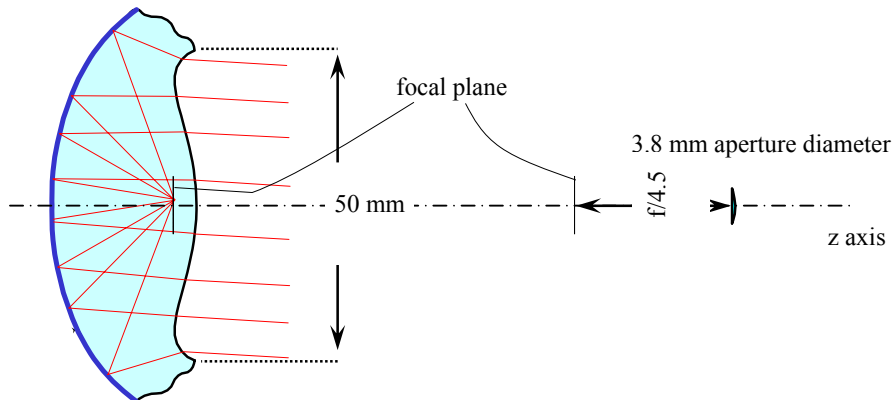


Figure 6. Example showing of the imaging properties of the RX. A 50-mm diameter RX (left) forms an image with the same quality (in terms of the MTF) than a conventional 3.8-mm diameter plano-convex lens (right) with $f/4.5$. Nevertheless the RX is 173 times more luminous. The numerical aperture of this RX is 1.46, i.e., 97.5% of the maximum theoretical NA. Refractive index $n=1.5$

the RX has an aperture 173 times bigger. The concentrating capability of the RX as an imaging device results in a numerical aperture (NA) of 1.46, i.e., a 97.5% of theoretical maximum.

The RXI is another SMS device that can be manufactured in a single dielectric piece (see Fig. 7). It has also two optical surfaces but, unlike the RX, the rays are deflected twice in one of the surfaces. Used also as a receiver, the rays coming from the source are first refracted at the first surface, then reflected at the second surface and then reflected again at the first surface. This last reflection is achieved by total internal reflection (TIR), except in a small central portion where TIR cannot be achieved. Owing to this, this central portion should be mirrored. This front mirror introduces some losses which, with a proper design, can be kept below 1%.

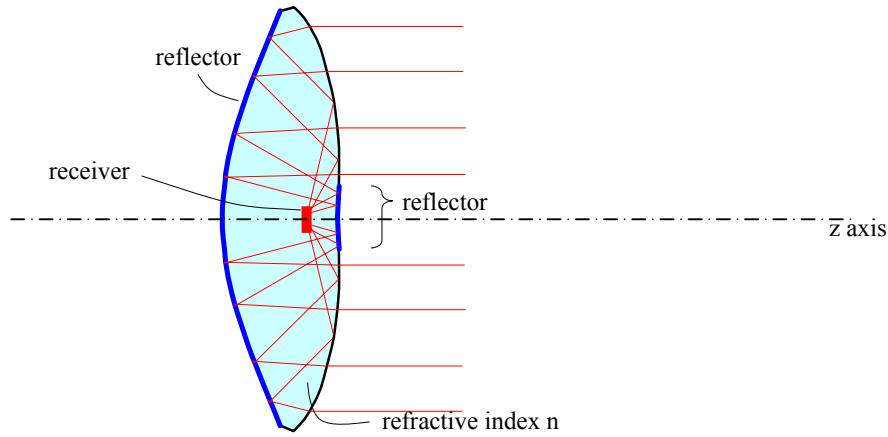


Figure 7. Cross-section of an RXI. Rays from the source are first refracted at the right-hand surface then reflected and finally reflected by total internal reflection at the right-hand surface. Total internal reflection cannot be achieved at the central points of this surface and thus this part should be mirrored. Refractive index $n=1.5$.

The angular transmission characteristic of the semiconductor surface should be also considered in the design in most cases because the goal is not to maximize the light on a receiver surface, for example, but to maximize the photocurrent. For instance, consider the design of a concentrator for a semiconductor receiver and assume a monochromatic source with even distribution of the incidence angle within the angular field of view ($\pm\theta_s$) and even distribution of the power in both polarization states. If the semiconductor-dielectric interface reflects the light reaching at gracing angles and we are interested in minimal receiver area, there is no use in illuminating the semiconductor in these directions. The concentrator output bundle may be restricted to some angular span $0-\theta_o$. Let us call $T_s(\alpha)$, the ratio of light power penetrating in the semiconductor to the power impinging the semiconductor surface at an incidence angle α with the surface's normal. In the designs shown in this paper, the receivers are assumed to have $T_s(\alpha)=1$. In a practical design $T_s(\alpha)<1$. An antireflection coating or the texturation of the semiconductor surface increases $T_s(\alpha)$. The optimization of the antireflection coating should be done considering isotropic illumination of the semiconductor and not a single incidence. In the case of minimal receiver's surface (maximal concentration) the variable to be optimized in the antireflection coating design is T_s , which is the ratio of power entering in the semiconductor to the power impinging isotropically its surface.

$$T_s = \int_0^{\pi/2} T_s(\alpha) \sin 2\alpha d\alpha \quad (3)$$

If the output bundle is restricted to $0-\theta_o$, then we have to optimize

$$T_s = \int_0^{\theta_o} T_s(\alpha) \sin 2\alpha d\alpha \quad (4)$$

The selection of the value of θ_0 will depend on the signal to internal noise ratio. Nonimaging tools also allows an easy consideration of the characteristics of the receiver (or the emitter)

4. RXI PROTOTYPE MEASUREMENTS

A series of RXI has been manufactured by injection molding of acrylic (PMMA). The entry aperture diameter is 40 mm and the design acceptance angle is ± 1.9 degrees (at 50% angular transmission). They are designed for a GaAs solar cell with a square $1 \times 1 \text{ mm}^2$ active area covered with a single-layer antireflective coating. The beam illuminating the cell is restricted to ± 70 degrees. More details of this prototype can be found in reference¹⁸.

The acrylic piece suffers an uneven shrinkage during the post injection cooling, which is the main source of errors in the accuracy of the optical surfaces. As an example of the values achievable with an inexpensive injection process, Figure 8 shows the difference in the z-coordinate between the theoretical values and the measured values of both optical surfaces.

Figure 9 shows the angular transmission. The theoretical angular transmission is calculated by ray-tracing and it gives the ratio of power reaching the receiver to the power impinging the entry aperture at a given incidence angle. This ray tracing can also be done with the measured data of the RXI surfaces (this result is also shown in Figure 9). The measured angular transmission is the normalized photocurrent when the RXI is homogeneously illuminated with a collimated beam that is falling on the entry aperture at a given angle. The photocurrent is normalized to the maximum value. This measured angular transmission is included in the same figure for illustration but it is not directly comparable with the other ones since it includes the effects of the semiconductor interface, the internal quantum efficiency and the collection efficiency.

Since the receiver is a square (and not a circle), the angular transmission has not rotational symmetry. In Figure 10, the emission diagram of this device is shown. This emission diagram has been obtained with a CCD camera capturing the radiation emitted by the RXI when the GaAs cell is in direct bias. This diagram is equivalent to the measured angular transmission, which, as said before, has no rotational symmetry. The angular transmission is function of two variables defining the direction of incoming rays. These two variables (p and q) are the direction cosines with respect two orthogonal axes (x and y) normal to the z-axis. The GaAs cell square sides are parallel to these axes. As it can be clearly seen in this figure, the angular transmission has also a square-like shape. The results of Figure 9 refers to the section $q=0$.

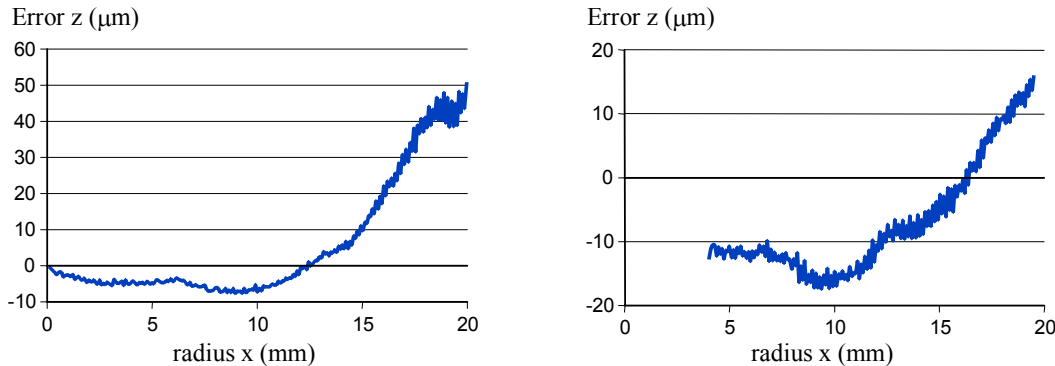


Figure 8. Left: Error in entrance aperture profile as a function of the distance to the axis of symmetry. Right: Back mirror profile error as a function of the distance to the axis of symmetry. In this surface the RXI has a hole in its center to allocate the cell.

The current gain is defined as the ratio of the photocurrent when the RXI is illuminated at normal incidence with a collimated beam to the photocurrent when the receiver is out of the concentrator. The maximum measured value in the prototype was 1100 times. The geometrical concentration (ratio of entry aperture area to receiver active area) is 1256.6. The geometrical concentration is not an upper bound of the current gain since the later includes the effects of index matching when the GaAs cell is within the concentrator.

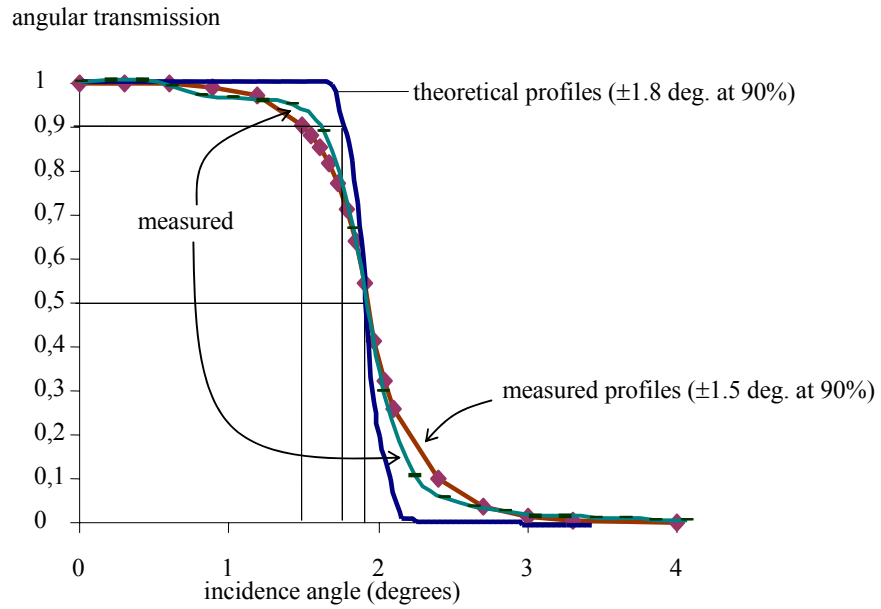


Figure 9. Angular transmission actually measured compared with the values obtained by ray tracing of the RXI with theoretical profiles and with the measured profiles. The measured acceptance angle is ± 1.6 degrees and the current gain is 1110.

At present, measurements are being carried out to get the amount of radiation impinging on the GaAs cell (and not the only radiation giving rise to photocurrent as has been done in the preceding measurements).

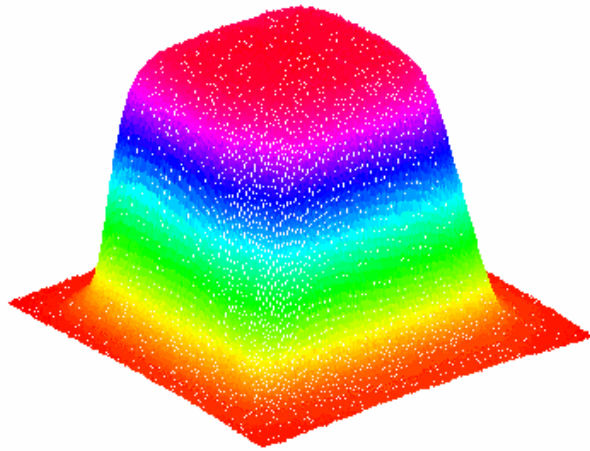


Figure 10. Angular emission diagram

5. CONCLUSIONS

Maximum efficient light transfer between a source and a receiver is the typical goal of a nonimaging design problem. This goal is also of interest in most wireless optical link design. An efficient concentration device allows smaller (and thus faster and less noisy) receivers. Nonimaging optics provides the tools for designing optical devices that perform very close to the thermodynamical limit of concentration. Moreover, the nonimaging designs have also applications in the emitters as collimators, particularly in those emitters, like the LED, where the light is emitted almost isotropically from the points of its surface.

Among the different nonimaging design methods, the SMS seems to be the most adequate for the type of problems found in wireless optical communications. The devices designed with the SMS method are simple, very compact, and provide room for easy placing the optoelectronic devices. Two of these devices have been shown: the RX and the RXI. Besides its nonimaging performance as a concentrator, the RX is also an imaging device with a very high numerical aperture (97.5% of the theoretical maximum) that has clear applications in highly sensitive focal plane arrays applications or in tracking sensors. The RXI stands out for its impressive compactness besides its capability for concentrating/collimating light.

For long range optical links applications, where the beam establishing the link has a small angular span, combinations of imaging and nonimaging devices are a convenient solution for diminishing the effects of the optical surfaces errors. In these cases, the Winston-Welford method or the combination of SMS and the WW methods also provide adequate solutions.

Nonimaging optics also provides the tools for other applications of wireless optical communication as the design of light efficient optical devices with prescribed angular emission (reception) characteristics.

ACKNOWLEDGEMENTS

This research was supported by the European JOULE program under contract JOR3-CT98-0252, contract TIC96-0725-C02-02 from the Plan Nacional de Investigación y Desarrollo with the Spanish Comisión Interministerial de Ciencia y Tecnología and contracts 06T/027/96 and 07T/0032/98 of the Consejería de Educación y Cultura of the Spanish Comunidad Autónoma de Madrid.

REFERENCES

- ¹ W.T. Welford, R. Winston. *High Collection Nonimaging Optics*, Academic Press, New York, 1989
- ² J.C. Miñano, "Design of three-dimensional nonimaging concentrators with inhomogeneous media", *J. Opt. Soc. Am. A*, 3(9), 1986, pp 1345-1353
- ³ J.C. Miñano, "Refractive index distribution in two-dimensional geometry for a given one-parameter manifold of rays", *J. Opt. Soc. Am. A*, 2, 1985, pp. 1821-1825
- ⁴ J.C. Miñano. "Poisson brackets method of design of nonimaging concentrators: a review" in *Nonimaging Optics: Maximum-Efficiency Light Transfer II*, Roland Winston, Robert L. Holman, Editors, Proc. SPIE 2016, 98-108 (1993)
- ⁵ R. Winston, *Nature*
- ⁶ P. Benítez, R. Mohedano, J.C. Miñano. "Manufacturing tolerances for nonimaging concentrators", in *Nonimaging Optics: Maximum Efficiency Light Transfer IV*, Roland Winston, Editor, Proc. SPIE vol. 3139, pp. 98-109 (1997). I.
- ⁷ J.C. Miñano, J. C. González. "Design of nonimaging lenses and lens-mirror combinations". SPIE's International Symposium on Optical Applied Science and Engineering. San Diego, California 1991, Proc. SPIE 1528 pp. 104-117. I.
- ⁸ J.C. Miñano, Juan C. González. "New Method of Design of Nonimaging Concentrators", *Applied Optics*, 31 (1992), pp. 3051-3060.
- ⁹ J.C. Miñano, P. Benítez, J.C. González. "RX: a Nonimaging Concentrator". *Applied Optics*, 34, 13 (1995), pp. 2226-2235.
- ¹⁰ J.C. Miñano, J.C. González, P. Benítez, "RXI: A high-gain, compact, nonimaging concentrator". *Applied Optics*, 34, 34 (1995), pp. 7850-7856.
- ¹¹ P. Benítez, R. García, J.C. Miñano, "Contactless efficient two-stage solar concentrator for tubular absorber". *Applied Optics*, 36, 28 (1997), pp. 7119-7128.
- ¹² P. Benítez, R. Mohedano, J.C. Miñano. "DSMTS: A novel linear PV concentrator". Proc. 26 IEEE Photovoltaic Specialists Conference. Anaheim, California, EEUU, 1997, pp. 1145-1148.

-
- ¹³ P. Benítez, R. Mohedano, J.C. Miñano, R. García, J.C. González. “Design of CPC-like reflectors within the simultaneous multiple surface design method”, in *Nonimaging Optics: Maximum Efficiency Light Transfer IV*, Roland Winston, Editor, Proc. SPIE vol. 3139, pp.19-28 (1997).
- ¹⁴ O.N. Stavroudis. *The Optics of Rays, Wavefronts, and Caustics*. Academic, New York, 1972
- ¹⁵ P. Benítez, R. Mohedano, J.C. Miñano. “Design in 3D geometry with the Simultaneous Multiple Surface design method of Nonimaging Optics”, in *Nonimaging Optics: Maximum Efficiency Light Transfer V*, Roland Winston, Editor, SPIE, Denver (1999).
- ¹⁶ P. Benítez, J.C. Miñano. “Ultra high numerical aperture imaging concentrator”. *J. Opt. Soc. of Am. A*, 14, 8 (1997), pp. 1988-1997.
- ¹⁷ R.K. Luneburg, *Mathematical Theory of Optics*, (University of California Press, Berkeley, 1964)
- ¹⁸ J. L. Álvarez, M. Hernández, P. Benítez, J.C. Miñano “RXI concentrator for 1000X photovoltaic energy conversion”, in *Nonimaging Optics: Maximum Efficiency Light Transfer V*, Roland Winston, Editor, SPIE, Denver (1999).